Preparation of Cellulosic Air Filters with Controllable Pore Structures *via* Organic Solvent-based Freeze Casting: The Key Role of Fiber Dispersion and Pore Size

Shanshan Ma,[a] Meiyun Zhang,[a,b] Bin Yang,[a,b] Shunxi Song,[a,c,*] Jingyi Nie,[a,*] and Peng Lu [c]

Green and biodegradable cellulose filters with controlled designer pore structures were prepared using organic solvent-based freeze casting. In this paper, the relationship between the different freeze media, including ethanol, isopropanol, and *tertiary*-butyl alcohol, and the microstructure of the porous filters was investigated. The results of the pore size distribution indicated that the pore channel size decreased remarkably when organic solvents were used as the freezing media. Moreover, the filters showed high filtration efficiencies, up to 99.70% and 99.66% for 0.5 μm and 0.3 μm particles, respectively, under a pressure drop of 180 Pa and at 32 $L \cdot min^{-1}$ flow rate. The fabrication of cellulosic filters would not only make it a promising candidate for capturing fine particulate matter, but also provide a versatile approach to regulate and design a porous structure for materials applied in various fields.

Keywords: Cellulosic air filters; Pore size; Organic solvent system; Freeze casting; Filtration performance

*Contact information: a: College of Bioresources Chemical and Materials Engineering, National Demonstration Center for Experimental Light Chemistry Engineering Education, Shaanxi University of Science & Technology, Xi'an, 710021, China; b: State Key Laboratory for Modification of Chemical Fibers and Polymer Materials, Donghua University, Shanghai, 201620, China; c: Guangxi Key Lab of Clean Pulp & Papermaking and Pollution Control, Guangxi University, Nanning, 530004, China; * Corresponding authors: 15829913710@163.com; jingyi.nie@163.com*

INTRODUCTION

Particulate air pollution (Brauer *et al.* 2016; Liang *et al.* 2016; Wu *et al.* 2017), especially fine particulate matter ($PM_{2.5}$, Aerodynamic equivalent diameter ≤ 2.5 μm), has intimate and severe impacts on human health (World Health Organization 2015), daily activities (Lee *et al.* 2015a), climate, and the environment (Brauer *et al.* 2012; Chafe *et al.* 2014). Additionally, statistics have shown that $PM_{2.5}$ concentration increments of 10 $\mu g/m^3$ on average can lead to an 8% and 6% increased risk in lung cancer and cardiopulmonary diseases, respectively (Pope III *et al.* 2002). Therefore, the urgent need for health assurance has drawn much attention to the exploration of high-performance air filters (Wan *et al.* 2014; Liu *et al.* 2017). Nowadays, porous membrane filters (Liu *et al.* 2011, 2015) and fibrous filters (MacFarlane *et al.* 2012) are common and popular in the market. However, the disposal of synthetic polymer-based filters results in secondary pollution because of their nonrenewable and non-degradable properties. In contrast to synthetic fibers, cellulosic fibers (Abdul Khalil *et al.* 2014; Lee *et al.* 2015b) may be a suitable candidate (Svagan *et al.* 2008) to fabricate renewable and sustainable filters. This suitability owes a great deal to the superior characteristics of the raw materials, such as their abundance in nature,

biodegradable sources, and low cost. Nevertheless, traditional cellulose filters cannot reach a satisfactory filtration performance because of their loose lamellar structure.

To obtain a satisfactory filtration performance, the filtration mechanism needs to be understood first. Generally, the model for the capture of particles is based on five filtration mechanisms (Zamani and Maini 2009; Sokovnin *et al.* 2015): physical sieving, interception, diffusion, inertial separation, and electrostatic attraction. Among these, physical sieving, interception, and diffusion usually play major roles in the filtration performance and largely depend on the pore size and structure (Zhao *et al.* 2017; Gong *et al.* 2018). Thus, regulating the pore size and structure is a key factor to improve the filtration performance of porous materials (Wang *et al.* 2009; Hu *et al.* 2010).

Freeze casting (Liu *et al.* 2013), is a versatile and promising method and is commonly employed to prepare porous materials with a sophisticated and hierarchical structure (Deville *et al*. 2006). This method could retain surface fibrillation of cellulose fibers and prevent the collapse of porous structure during the drying process (Mao *et al.* 2008). The designed microstructures of porous materials are controlled by several parameters (Qian and Zhang 2011; Waschkies *et al.* 2011), including the freezing temperature, pulp consistency, and freezing medium. Different freezing media (Cui *et al.* 2006; Nemoto *et al.* 2015) remarkably influence the pore structure and size of materials by altering the growth behavior of crystals (Teagarden and Baker 2002; Dong *et al.* 2017). Moreover, the pore structure of the samples is the reverse replication of the shape of solvent crystals during the freeze-drying process (Deville 2008). Therefore, choosing a suitable freezing medium is the key step in fabricating air filters with excellent filtration performances.

Suitable freezing media, such as water, camphene, and *tertiary*-butyl alcohol (TBA), have been successfully used in the fabrication of air filters. Water has widely been applied in the ice-templating synthesis of porous materials because it is low-cost and harmless to the environment (Gutiérrez *et al.* 2008). Unlike the lamellar or dendritic structure of water or camphene-based crystals, an organic eutecticum generally exhibits a long straight prism and would be beneficial for fabricating filters with a dense structure applied in the intercepting of PM (Oesterle *et al.* 1998; Wittaya-Areekul and Nail 1998). Additionally, using organic solvents as freezing media could shorten the sublimation time and decrease the energy consumption because of a high equilibrium vapor pressure and low surface tension (Kasraian and DeLuca 1995). Ethanol and isopropanol were also used to fabricate cellulose fiber-based filters in this study because of the similarity of the chemical structures. Cao *et al.* (2013) fabricated regenerated silk fibroin scaffolds with controllable porous three-dimensional microstructures with the addition of n-butanol. Sehaqui *et al.* (2011) produced an aerogel with a specific surface area as high as 153 m^2/g to 284 m^2/g according to the solvent exchange method from water to TBA. Miller *et al.* (2015) found that the pore size was related to the specific freezing medium in the alumina ceramics fabrication process. This means it provides a desirable method to prepare filters with a controllable pore morphology (Vessot and Andrieu 2012).

The objective of this research is to explore a means of preparing biodegradable cellulose air filters with various pore structures based on organic solvent-water miscible systems *via* freeze casting. Ethanol, isopropanol, and TBA were employed to regulate the microstructures of the filters. The effects of different alcohols and content of TBA on the pore morphology, pore size distribution, porosity, specific surface area, and filtration performance of the filter samples were investigated. Furthermore, the regulating mechanisms of the alcohols on the pore structure and size of the filters were also

investigated and discussed. This work provides a useful way to fabricate renewable and sustainable air filters with controllable pore structures and displays a great potential in PM removal and air purification. Moreover, the results give a deep insight into the structure-property relationship of cellulose filters during freeze casting.

EXPERIMENTAL

Materials

Air-dried softwood Kraft pulp board with a solids content of 95.5% was obtained from Shan Dong Pulp & Paper Co., Ltd (Jinan, China). Analytical grade TBA, isopropyl alcohol, and ethanol were purchased from Tianjin Damao Chemical Reagent Company (Tianjin, China).

Methods

Preparation of the cellulosic air filters

A softwood pulp board (30 g, oven-dried) was immersed in water for 24 h to obtain swollen and flexible fibers, which were then disintegrated with a Lorentzen & Wettre disperser (Sartorius, Göttingen, Germany) at 12000 rpm. The fiber pulp at 10% (w/w) was further treated using a KPK PFI Refiner (Kumagai Riki Kogyo, Tokyo, Japan) at 10000 rpm, 20000 rpm, 30000 rpm, 40000 rpm, and 50000 rpm to obtain fibrillated cellulosic fibers. A schematic illustration for fabricating the high performance cellulosic air filters *via* freeze-drying is shown in Fig. 1.

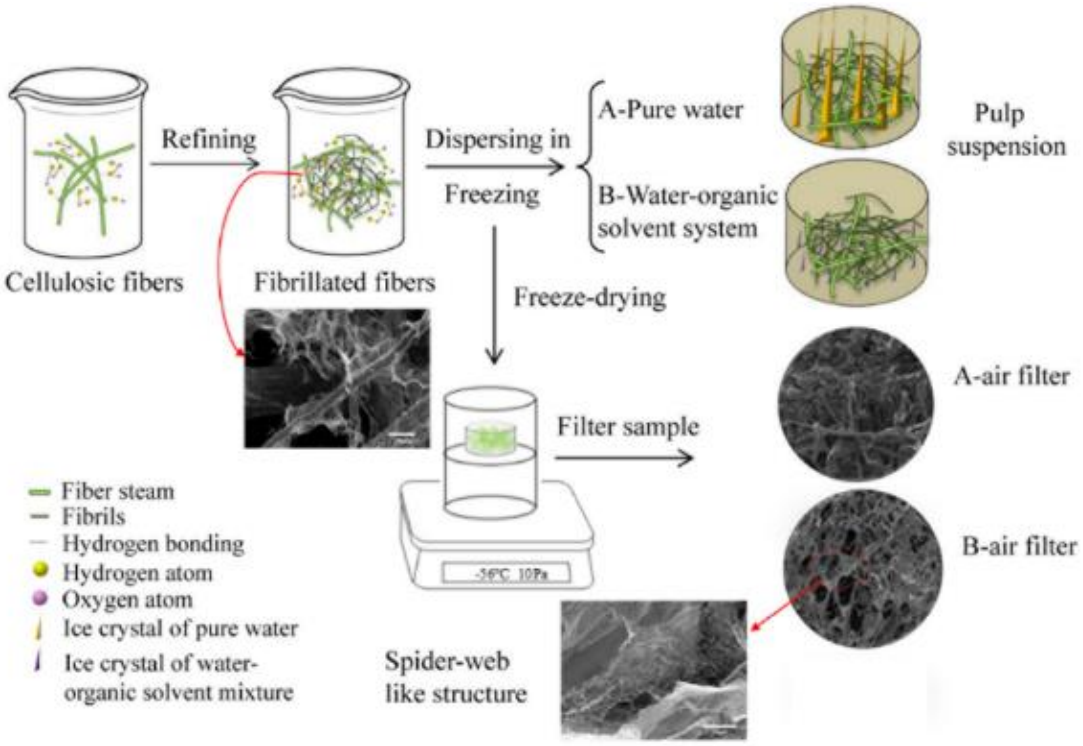

Fig. 1. Schematic illustration for preparing the air filters

The fibrillated fibers treated by the refining process were dispersed in different media (A - Purified water; B - Water with ethanol, isopropanol, or 10% v/v TBA) to obtain a uniform pulp suspension. The addition of ethanol and isopropanol in this study was under 10% (v/v) to ensure that the samples were completely frozen. This was done to avoid the "partial cake collapse" phenomenon (Daoussi *et al.* 2009) that occurs when the content of ethanol and isopropanol is over 10% (v/v) because of the low freezing points of these alcohols. Then, the 1.5% (w/w) suspension was poured into a petri dish and kept at -56 °C for 4 h. Finally, the samples were placed in a BILON freeze dryer (Shanghai Bilang Instrument Manufacture Co. Ltd., Shanghai, China) to sublimate and remove the residual solvent at -56 °C under 10 Pa for 3 d. The A-air filter was based on purified water and presented a layered structure. The B-air filter was prepared with an organic solvent and presented a porous architecture with a spider web-like structure.

The filtration performance was measured with an automated filter tester (LZC-K, Suzhou Huada Filter Technology Co. Ltd., Suzhou, China) according to European standard EN 1822-3:2000, which consisted of an aerosol generator, laser particle counter (2.83 L/min), flow counter (5 L/min to 50 L/min), spray pump (80 L/min, 220 V), and a pair of filter holders with a diameter of 10 cm. The filter tester was equipped with a diethyl hexyl sebacate (DEHS) aerosol nebulizer for generating fine particles (PMs) with the diameter of 300 nm to 500 nm (Thiessen 2006). The flow rate though air filter, total measuring time, relative humidity, and temperature were set to 32 L/min, 10 s, room temperature (25 °C), and 40% RH during testing process, respectively. The consistency of PMs in airflow after filtration testing was detected by a particle counter. And the pressure change of airflow was measured using a pressure detector. The filtration efficiency and pressure drop were employed to evaluate the filtration performance of the filter samples. The filtration efficiency (η) was calculated from the upstream and downstream particle concentrations using Eq. 1,

$$\eta = 1 - \frac{C_{\text{downstream}}}{C_{\text{upstream}}} \quad (1)$$

where $C_{\text{downstream}}$ is the downstream particle concentration (%) and C_{upstream} is the upstream particle concentration (%).

The pressure drop (ΔP) was determined from the upstream and downstream pressures with Eq. 2,

$$\Delta P = P_{\text{upstream}} - P_{\text{downstream}} \quad (2)$$

where $P_{\text{downstream}}$ is the downstream pressure (Pa) and P_{upstream} is the upstream pressure (Pa).

The quality factor (QF) is a typical index to evaluate the filtration performance. The QF (MacFarlane *et al.* 2012) value was independent of the porosity and thickness of the samples, and was calculated with the following formula:

$$QF = \frac{-\ln(1 - \eta)}{\Delta P} \quad (3)$$

The surface morphology of the fibrillated fibers and filter samples were sputter-coated with gold and observed with scanning electron microscopy (SEM) (VEGA-3-SBH, TESCAN, Brno, Czech Republic) at an operating voltage of 10 kV.

The Brunauer–Emmett–Teller specific surface area (BET-SSA) of the filter samples was calculated with N_2 adsorption isotherms using a Gemini VII2390 automated apparatus (Micromeritics, Shanghai, China) at a relative vapor pressure of 0.01 MPa to 0.3 MPa (Sehaqui *et al.* 2011). Samples (0.1 g to 0.2 g) were degassed with N_2 at 105 °C for 1 h before N_2 adsorption testing occurred at -196 °C.

The porosity reflects the density of the samples, which refers to the ratio of the total volume of the micropores to the volume of the porous materials (Sehaqui *et al.* 2011). The porosity and distribution of the pore size was analyzed with a Mercury Intrusion Porosimeter (AutoPore-IV9500, Micromeritics, Shanghai, China).

RESULTS AND DISCUSSION

Effects of the Organic Solvent-water Systems on the Pore Size and Structure

Figure 2 shows digital photographs and SEM images of the air filters prepared with different freezing media, including water, ethanol, isopropanol, and TBA. Figures 2a and 2e show that with purified water as the freezing medium the filter samples presented a rough surface at the macro level and a lamellar structure at the micro level. This morphology was attributed to the growth of ice crystals in a certain direction. Moreover, undesirable phenomena often occurred during the drying process because of strong surface tension and capillary action. These phenomena included the collapse of fiber-network (Mao *et al.* 2009) and slight shrinkage of the samples. Hence, the filters based on purified water usually showed a poor filtration efficiency because of the large-sized pores and damaged structure. Therefore, organic solvents were employed to improve the filtration performance of the samples (Fig. 2). The filtration performance could be improved with regards to the microstructure, pore size distribution, and porosity (Nemoto *et al.* 2015). A transformation of the sample structure from anisotropic to isotropic was observed (Figs. 2i to 2l). The samples prepared with the water/ethanol system presented a cellular structure because of the existence of hydrogen bonding (Figs. 2b, 2f, and 2j). The samples prepared with a water/isopropanol system presented regular pores with a fine network structure built by fiber trunks and fibrils (Fig. 2c, 2g, and 2k). Moreover, the samples prepared with a water/TBA system presented smaller sized pores than those based on the other solvents (Figs. 2d, 2h, and 2l). These types of three-dimensional filters showed uniform and smooth surfaces with a spider web-like structure. These networks and spider web-like structures greatly contributed to increasing the filtration performance of the samples.

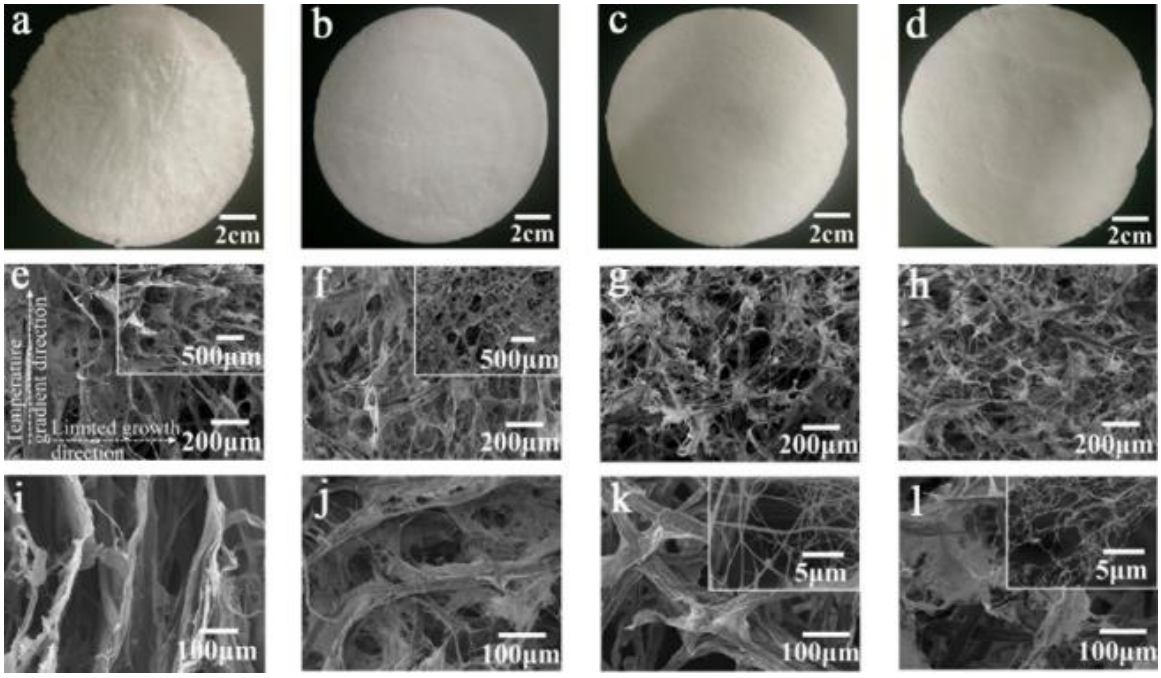

Fig. 2. Samples and SEM images of the air filters prepared with different freezing media: (a, e, and i) purified water; (b, f, and j) water/ethanol system; (c, g, and k) water/isopropanol system; and (d, h, and l) water/TBA system

The pore size and distribution of the cellulosic filters directly affect the filtration efficiency. Figure 3a shows the pore size distribution of the filter samples prepared with water, ethanol, isopropanol, and TBA, which was in the range of 5 μm to 200 μm with peaks centered at 120.9 μm, 90.8 μm, 90.8 μm, and 72.6 μm, respectively. Numerous large pores were clearly observable, which were formed by the fiber trunk, while the pores under 10 μm in size were constructed by fibrils. In fact, the peak at 6.0 μm was relative to the spider web-like structure in the filters based on TBA. Moreover, the pore size distribution of the filters based on the organic solvent systems showed a wider tendency and the peak shifted towards a smaller size gradually compared with that based on purified water. Moreover, the BETSSA results of the samples (Fig. 3b) were in good agreement with the tendency shown by the pore area. In addition to the pore size and distribution, the porosity is commonly used to evaluate the porous structure. Figure 3c shows the porosity of the filter samples prepared with different freezing media. The porosity of the filter samples increased mildly from 94.8% to 96.4% when the freezing media was changed from purified water to TBA. This was likely the result of the fixed freezing temperature and suspension concentration. The above results displayed that adopting alcohol molecules as the freezing medium had certain effects on regulating and controlling the distribution and size of the pores. Meanwhile, the improvement was gradually enhanced in the order of ethanol, isopropanol, and TBA.

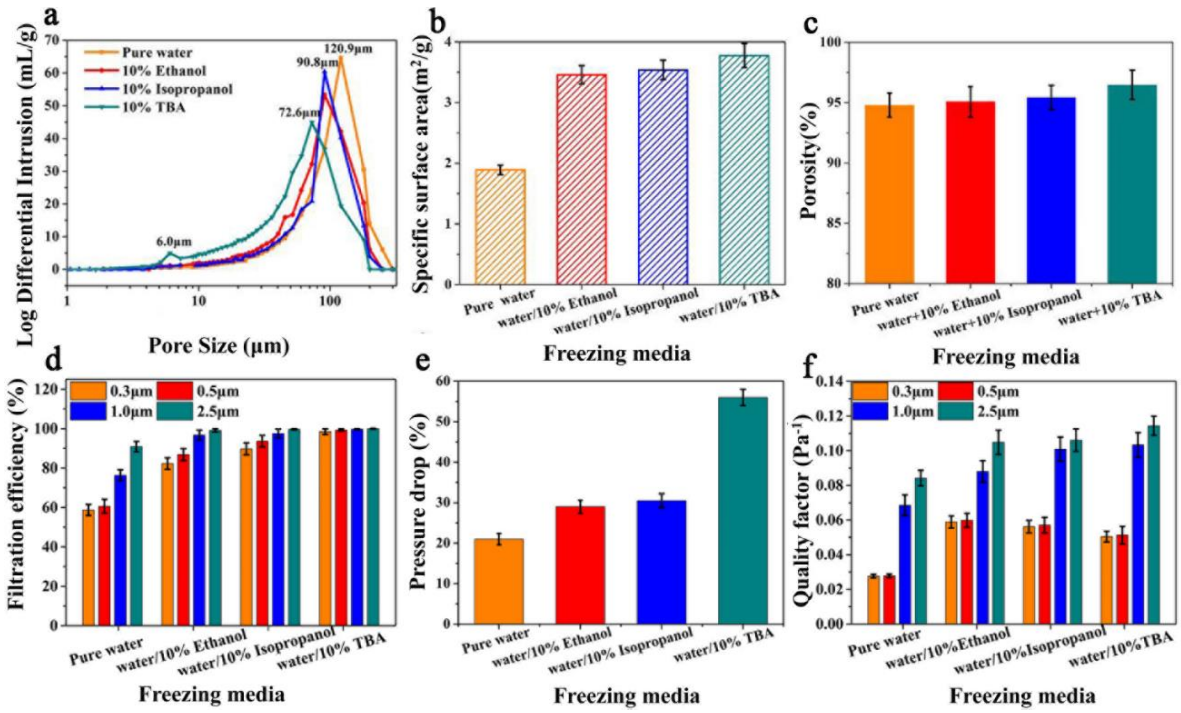

Fig. 3. (a) Pore size distribution; (b) Specific surface area; (c) Porosity; (d) Filtration efficiency; (e) Pressure drop; and (f) Quality factor of the filter samples prepared with different freezing media

The size and structure of the pores play essential roles in the filtration performance of air filters because of the sieving, interception, and diffusion mechanisms. Yang *et al.* (2015) reported that composite membranes could trap most of the particles by sieving with a narrow pore distribution. Figures 3d and 3e show that the filtration efficiency and pressure drop of the air filters presented an upward tendency with organic solvents as the freezing medium. Different particulates were applied during testing to evaluate the filtration performance, with average sizes of 0.3 μm, 0.5 μm, 1.0 μm, and 2.5 μm. The air filter prepared with water/10% TBA reached a filtration efficiency of 94.4% and 94.1% for the 0.5 μm and 0.3 μm particles, respectively, under a pressure drop of 56 Pa. Because of the net structure, the enhancement of the effective collision that occurred between the filters and fine particles resulted in a noticeable improvement in the interception and capture capability. Furthermore, the QF, as a comprehensive parameter, was introduced in the present work to evaluate the filtration performance (Fig. 3f). Generally, a higher QF value represents a greater filtration performance. The QF value indicated that the filters based on organic solvents had a better performance than that based on purified water. Thus, adopting water/organic solvent systems as the freezing medium effectively improved the ability of the air filters to capture particles.

Mechanistic Explanation of the Pore Size

Figure 4a shows that the water crystallized to form unidirectionally aligned ice layers because the growing velocity of the ice front along the temperature gradient was 100 to 1000 times higher than that in the vertical direction (Deville 2008). Generally, the transition from a planar to lamellar structure of ice crystals happens at a high solids content. Waschkies *et al.* (2011) explained that increasing solids content would cause super-cooling of the liquid and lower thermodynamic solidification rate lead to approaching critical rate

for the transition. Finally, the volatile planar ice front triggered the formation of the lamellar microstructure gradually. Figure 2i shows the lamellar porous structure of the filters, which was because of the repulsive force from the ice crystals. Nevertheless, an anisotropic and lamellar structure with large-sized pores was not good for catching particles.

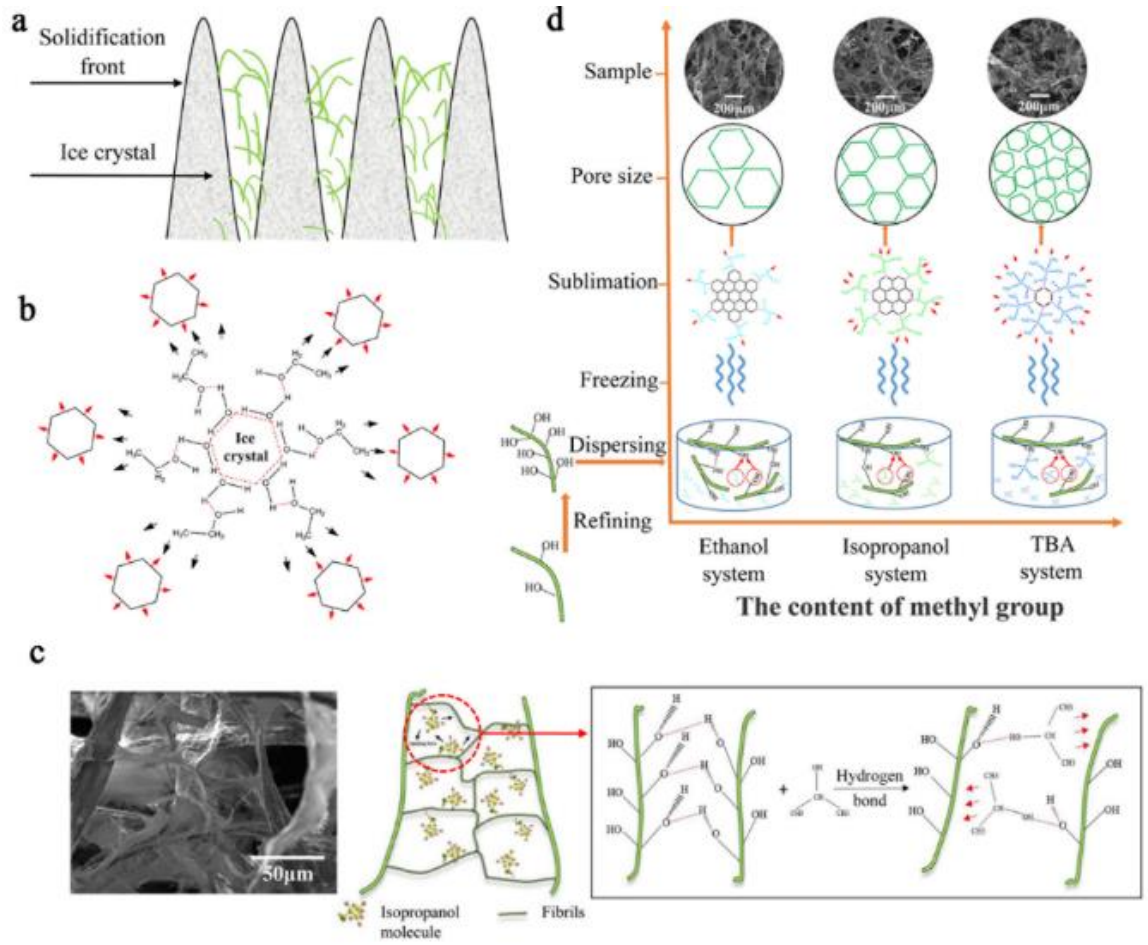

Fig. 4. Schematic diagram of (a) Growth process of the lamellar ice crystals (Waschkies *et al*. 2011); (b) Growth of ice crystal limited by ethanol molecules; (c) Disruption of hydrogen bonding by isopropanol molecules; and (d) Pore structure of the filter samples prepared with various freezing media

The effects of alcohols on regulating the pore structure and size can be understood based on the following mechanisms. First, the hydroxyl group at one end of the alcohol chain combined with water molecules to form eutectic compounds, and the methyl groups at the other end had a slight repulsive force on other hexagonal crystals. This inhibitory effect could have prevented the formation of large-sized ice crystals. The addition of alcohols would seize hydroxyl active sites of fibrillated fibers and form hydrogen bonding with fibers, which would have resulted in the generation of numerous tiny pores. Moreover, alcohols could improve the flocculation of fibrils in suspension. Second, the alcohols seized hydroxyl active sites on the surface of fibrillated fibers and weakened the bonding between the fibrils because of a steric effect, which could have effectively alleviated the flocculation of fibrils.

Figure 4b reveals that the growth of hexagonal crystals was limited by ethanol molecules. Because of the repulsive force, the eutectic crystals were smaller than that of the ice crystals based on purified water (Kasraian and DeLuca 1995; Wang *et al*. 2010). Also, the pore sizes of the filters were in good agreement with the tendency of the crystal sizes. It was observed that the pore size of the sample prepared with the ethanol/water system (90.8 μm) was smaller than that with purified water (120.9 μm) (Fig. 3a). Thus, the alcohol molecules affected the growth of ice crystals and had a certain inhibitory effect on the size of the ice crystals. Figure 4c illustrates the dispersion effect on the fibrils with the addition of isopropanol molecules. Generally, the filter sample based on purified water presented large-sized pores, which were mainly built by the fiber trunk. Large amounts of fibrils were wasted because of a flocculation phenomenon. When isopropanol molecules were employed, the degree of accessibility of hydrogen bonding between fibrils was decreased because of a steric effect. The bonding between the fibrils was weakened and partly interrupted, which led to the alleviation of fibrils flocculation. The schematic illustration for preparing cellulosic air filters with controllable pore structures based on various organic solvent systems is shown in Fig. 4d. After ethanol, isopropanol, and TBA were introduced, each alcohol molecule would bond to the free hydroxyl on the surface of fibrillated fibers. The process could hinder the bonding between fibers and effectively alleviate the excessive flocculation phenomenon of fibers (Jiang and Hsieh 2014). The increase in methyl groups caused steric hindrance and formed a more homogeneous slurry suspension. A decreasing trend in the pore size was observed under the comprehensive influence of the enhanced inhibitory effect and steric hindrance. Furthermore, the degree of undercooling in the mixed solution increased and the surface tension of the suspension decreased with the addition of alcohols. A high undercooling degree led to the formation of more fine crystals and resulted in the fabrication of filters with an abundance of micropores (Wang *et al.* 2010). Therefore, the introduction of alcohols played an effective role in regulating the pore size of the filter samples.

Effect of the TBA Content on the Pore Structure and Filtration Performance of the Air Filters

The morphology, specific surface area, pore size, and area of the samples prepared with different TBA contents are shown in Fig. 5. As the TBA content increased, the inhibitory effect of the TBA on the growth of ice crystals was enhanced, which resulted in the transformation of the crystal structure from a thick to thin needle-like shape. In particular, the eutectic crystals based on 90% TBA presented a small size, similar to what Vessot and Andrieu (2012) reported.

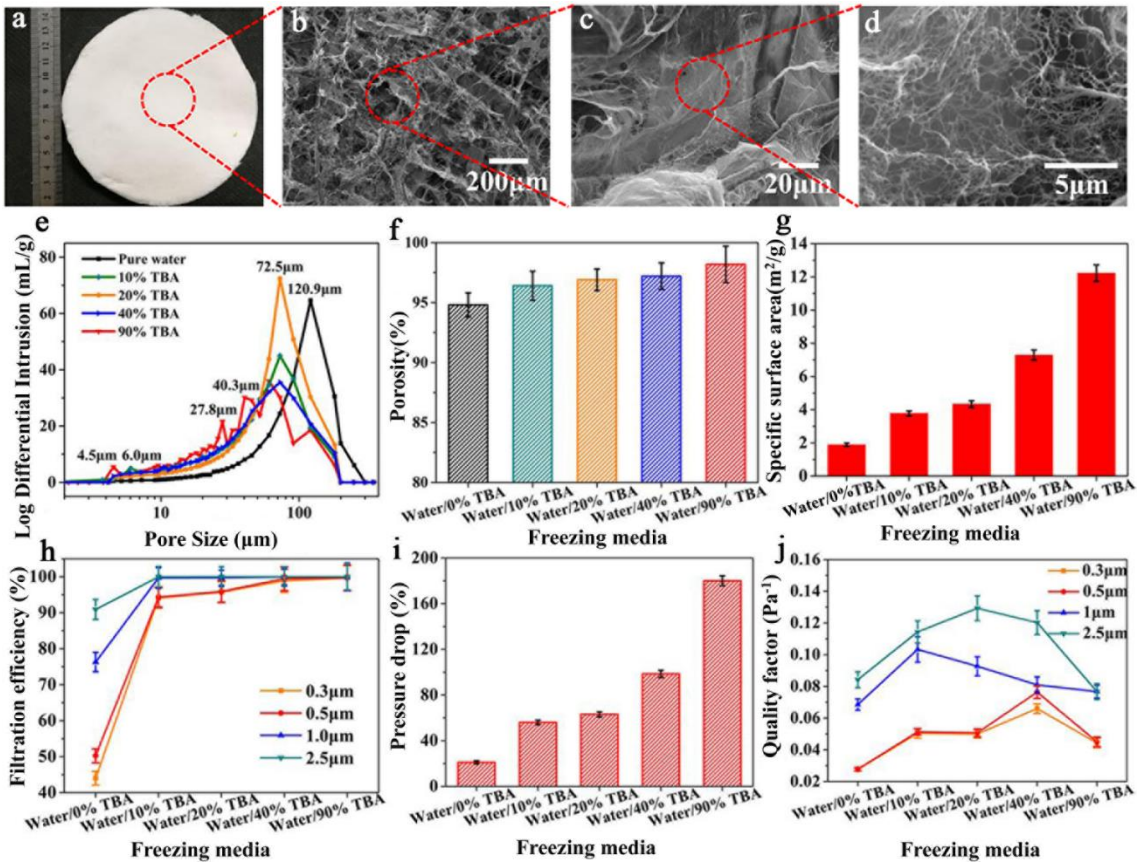

Fig. 5. (a) Sample and (b, c, and d) SEM images prepared with 90% TBA; (e) Pore size distribution; (f) Porosity; (g) Specific surface area contents; (h) Filtration efficiency; (i) Pressure drop; and (j) Quality factor of the filters prepared with different contents of TBA solution

The eutectic crystals in Fig. 2 were consistent with that of the ice crystal model that is shown in Fig. 4d. Figures 5a to 5d show the sample and SEM images prepared with 90% TBA. The spider web-like structure can be clearly observed in Figs. 5c and 5d. This special structure was beneficial for intercepting and capturing more fine particles. Additionally, the pore distribution exhibited a wider trend with an increase in the TBA content. The pore peaks of the filters prepared with 90% TBA were centered at 60.5 μm, 40.3 μm, 27.8 μm, and 4.5 μm (Fig. 5e). The tendency of the porosity and specific surface area also supported the pore size distribution of the filters. The porosity of the filters reached 98.2% when 90% TBA was used as the freezing medium (Fig. 5f). The specific surface area of the samples remarkably improved by 318% when the content of TBA increased from 0% to 90% (Fig. 5g). Thus, the filters based on 90% TBA had great potential for intercepting $PM_{2.5}$ because of the spider web-like structure and high specific surface area.

The filtration performance of the air filters prepared with different TBA contents is shown in Figs. 5h to 5j. By adding TBA, a spider web-like structure developed because of the strong steric and inhibitory effects (Fig. 5d). The spider web-like structure contributed to the capture and interception of particles. Compared with the filters based on purified water, the filters based on 90% TBA showed excellent filtration efficiencies. The filtration efficiency was 99.7% and 99.7% for 0.5 μm and 0.3 μm particles, respectively, under a 180 Pa pressure drop and at 32 $L \cdot min^{-1}$ flow rate (Figs. 5h to 5i). With an increase in the TBA content, both the filtration efficiency and pressure drop showed upward trends. The

improved filtration efficiency and large pressure drop was attributed to the narrowed pore size. Figure 5j shows that the QF increased to a maximum value of 0.076 Pa^{-1} and 0.066 Pa^{-1} for the 0.5 μm and 0.3 μm particles, respectively, when 40% TBA was used as the freezing medium. Then, the QF decreased because of the sharp increase in the pressure drop. Therefore, with respect to high QFs, the filters based on 40% TBA would have an excellent filtration performance with a low resistance and ultra-high capture efficiency.

CONCLUSIONS

1. Green and biodegradable air filters with controllable pore structures and excellent filtration efficiencies were prepared with organic solvent systems *via* the freeze casting technique. Moreover, the pore size of filters decreased obviously due to the enhanced inhibitory effect when the freezing media was changed in the order of ethanol, isopropanol, and TBA.
2. When 90% (v/v) TBA was used as the freezing medium, the pore size of the filters decreased from 120.9 μm to 60.5 μm, 40.3 μm, 27.8 μm, and 4.5 μm, which led to the formation of a spider web-like structure. Moreover, the filtration efficiency was as high as 99.7% and 99.7% for the 0.5 μm and 0.3 μm particles, respectively. Additionally, this work provides a guide for promoting the use of cellulosic filter materials in practical applications.

ACKNOWLEDGMENTS

This research was supported by National Key R&D Program of China (2017YFB0308300), the State Key Laboratory for modification of chemical fibers and polymer materials, Donghua University (LK1601), National Science Foundation of China (31670593), Guangxi Key Laboratory of Clean Pulp & Papermaking and Pollution Control (KF201701). The authors would like to thank Suzhou Huada Instrument and Equipment Ltd. (China) for help with particle testing. The useful suggestions from the anonymous reviewers were also greatly appreciated.

REFERENCES CITED

Abdul Khalil, H. P. S., Davoudpour, Y., Islam, M. N., Mustapha, A., Sudesh, K., Dungani, R., and Jawaid, M. (2014). "Production and modification of nanofibrillated cellulose using various mechanical processes: A review," *Carbohyd. Polym.* 99, 649-665. DOI: 10.1016/j.carbpol.2013.08.069

Brauer, M., Amann, M., Burnett, R. T., Cohen, A., Dentener, F., Ezzati, M., Henderson, S. B., Krzyzanowski, M., Martin, R. V, Van Dingenen, R., *et al*. (2012). "Exposure assessment for estimation of the global burden of disease attributable to outdoor air pollution," *Environ. Sci. Technol.* 46(2), 652-660. DOI: 10.1021/es2025752

Brauer, M., Freedman, G., Frostad, J., van Donkelaar, A., Martin, R. V., Dentener, F., van Dingenen, R., Estep, K., Amini, H., Apte, J. S., *et al.* (2016). "Ambient air pollution exposure estimation for the global burden of disease 2013," *Environ. Sci. Technol.* 50(1), 79-88. DOI: 10.1021/acs.est.5b03709

Cao, Z., Wen, J., Yao, J., Chen, X., Ni, Y., and Shao, Z. (2013). "Facile fabrication of the porous three-dimensional regenerated silk fibroin scaffolds," *Mat. Sci. Eng. C-Mater.* 33(6), 3522-3529. DOI: 10.1016/j.msec.2013.04.045

Chafe, Z. A., Brauer, M., Klimont, Z., Van Dingenen, R., Mehta, S., Rao, S., Riahi, K., Dentener, F., and Smith, K. R. (2014). "Household cooking with solid fuels contributes to ambient $PM_{2.5}$ air pollution and the burden of disease," *Environ. Health Persp.* 122(12), 1314-1320. DOI: 10.1289/ehp.1206340

Cui, J., Li, C., Deng, Y., Wang, Y., and Wang, W. (2006). "Freeze-drying of liposomes using tertiary butyl alcohol/water cosolvent systems," *Int. J. Pharm.* 312(1-2), 131-136. DOI: 10.1016/j.ijpharm.2006.01.004

Daoussi, R., Vessot, S., Andrieu, J., and Monnier, O. (2009). "Sublimation kinetics and sublimation end-point times during freeze-drying of pharmaceutical active principle with organic co-solvent formulations," *Chem. Eng. Res. Des.* 87(7), 899-907. DOI: 10.1016/j.cherd.2008.09.007

Deville, S. (2008). "Freeze-casting of porous ceramics: A review of current achievements and issues," *Adv. Eng. Mater.* 10(3), 155-169. DOI: 10.1002/adem.200700270

Deville, S., Saiz, E., Nalla, R. K., and Tomsia, A. P. (2006). "Freezing as a path to build complex composites," *Science* 311(5760), 515-518. DOI: 10.1126/science.1120937

Dong, S., Wang, L., Gao, X., Zhu, W., Wang, Z., Ma, Z., and Gao, C. (2017). "Freeze casting of novel porous silicate cement supports using tert-butyl alcohol-water binary crystals as template: Microstructure, strength and permeability," *J. Membrane Sci.* 541, 143-152. DOI: 10.1016/j.memsci.2017.06.067

Gong, J., Stewart, M. L., Zelenyuk, A., Strzelec, A., Viswanathan, S., Rothamer, D. A., Foster, D. E., and Rutland, C. J. (2018). "Importance of filter's microstructure in dynamic filtration modeling of gasoline particulate filters (GPFs): Inhomogeneous porosity and pore size distribution," *Chem. Eng. J.* 338, 15-26. DOI: 10.1016/j.cej.2018.01.006

Gutiérrez, M. C., Ferrer, M. L., and del Monte, F. (2008). "Ice-templated materials: Sophisticated structures exhibiting enhanced functionalities obtained after unidirectional freezing and ice-segregation-induced self-assembly," *Chem. Mater.* 20(3), 634-648. DOI: 10.1021/cm702028z

Hu, L., Wang, C.-A., Huang, Y., Sun, C., Lu, S., and Hu, Z. (2010). "Control of pore channel size during freeze casting of porous YSZ ceramics with unidirectionally aligned channels using different freezing temperatures," *J. Eur. Ceram. Soc.* 30(16), 3389-3396. DOI: 10.1016/j.jeurceramsoc.2010.07.032

Jiang, F., and Hsieh, Y.-L. (2014). "Assembling and redispersibility of rice straw nanocellulose: Effect of *tert*-butanol," *ACS Appl. Mater. Inter.* 6(22), 20075-20084. DOI: 10.1021/am505626a

Kasraian, K., and DeLuca, P. P. (1995). "Thermal analysis of the tertiary butyl alcohol-water system and its implications on freeze-drying," *Pharm. Res.* 12(4), 484-490. DOI: 10.1023/A:1016233408831

Lee, E. S., Fung, C.-C. D., and Zhu, Y. (2015a). "Evaluation of a high efficiency cabin air (HECA) filtration system for reducing particulate pollutants inside school buses," *Environ. Sci. Technol.* 49(6), 3358-3365. DOI: 10.1021/es505419m

Lee, S. H., Lee, H. L., and Youn, H. J. (2015b). "Adsorption of xylan onto cellulose fibers pretreated with cationic polyelectrolyte and its effect on paper properties," *BioResources* 10(1), 851-865. DOI: 10.15376/biores.10.1.851-865

Liang, C.-S., Duan, F.-K., He, K.-B., and Ma, Y.-L. (2016). "Review on recent progress in observations, source identifications and countermeasures of $PM_{2.5}$," *Environ. Int.* 86, 150-170. DOI: 10.1016/j.envint.2015.10.016

Liu, C., Hsu, P. C., Lee, H. W., Ye, M., Zheng, G., Liu, N., Li, W., and Cui, Y. (2015). "Transparent air filter for high-efficiency $PM_{2.5}$ capture," *Nat. Commun.* 6, 1-9. DOI: 10.1038/ncomms7205

Liu, J., Pui, D. Y. H., and Wang, J. (2011). "Removal of airborne nanoparticles by membrane coated filters," *Sci. Total Environ.* 409(22), 4868-4874. DOI: 10.1016/j.scitotenv.2011.08.011

Liu, J., Zhang, X., Zhang, H., Zheng, L., Huang, C., Wu, H., Wang, R., and Jin, X. (2017). "Low resistance bicomponent spunbond materials for fresh air filtration with ultra-high dust holding capacity," *RSC Adv.* 7(69), 43879-43887. DOI: 10.1039/C7RA07694K

Liu, R., Yuan, J., and Wang, C.-a. (2013). "A novel way to fabricate tubular porous mullite membrane supports by TBA-based freezing casting method," *J. Eur. Ceram. Soc.* 33(15-16), 3249-3256. DOI: 10.1016/j.jeurceramsoc.2013.06.005

MacFarlane, A. L., Kadla, J. F., and Kerekes, R. J. (2012). "High performance air filters produced from freeze-dried fibrillated wood pulp: Fiber network compression due to the freezing process," *Ind. Eng. Chem. Res.* 51(32), 10702-10711. DOI: 10.1021/ie301340q

Mao, J., Grgic, B., Finlay, W. H., Kadla, J. F., and Kerekes, R. J. (2008). "Wood pulp based filters for removal of sub-micrometer aerosol particles," *Nord. Pulp Pap. Res. J.* 23(4), 420-425. DOI: 10.3183/NPPRJ-2008-23-04-p420-425

Mao, J. L., Kadla, J. F., and Kerekes, R. J. (2009). "Retaining surface fibrillation of wet-beaten wood pulp in the dry state," *Tappi J.* 8(7), 25-30.

Miller, S. M., Xiao, X., and Faber, K. T. (2015). "Freeze-cast alumina pore networks: Effects of freezing conditions and dispersion medium," *J. Eur. Ceram. Soc.* 35(13), 3595-3605. DOI: 10.1016/j.jeurceramsoc.2015.05.012

Nemoto, J., Saito, T., and Isogai, A. (2015). "Simple freeze-drying procedure for producing nanocellulose aerogel-containing, high-performance air filters," *ACS Appl. Mater. Inter.* 7(35), 19809-19815. DOI: 10.1021/acsami.5b05841

Oesterle, J., Franks, F., and Auffret, T. (1998). "The influence of tertiary butyl alcohol and volatile salts on the sublimation of ice from frozen sucrose solutions: Implications for freeze-drying," *Pharm. Dev. Technol.* 3(2), 175-183. DOI: 10.3109/10837459809028493

Pope III, C. A., Burnett, R. T., Thun, M. J., Calle, E. E., Krewski, D., Ito, K., and Thurston, G. D. (2002). "Lung cancer, cardiopulmonary mortality, and long-term exposure to fine particulate air pollution," *JAMA-J. Am. Med. Assoc.* 287(9), 1132-1141. DOI: 10.1001/jama.287.9.1132

Qian, L., and Zhang, H. (2011). "Controlled freezing and freeze drying: A versatile route for porous and micro-/nano-structured materials," *J. Chem. Technol. Biot.* 86(2), 172-184. DOI: 10.1002/jctb.2495

Sehaqui, H., Zhou, Q., and Berglund, L. A. (2011). "High-porosity aerogels of high specific surface area prepared from nanofibrillated cellulose (NFC)," *Compos. Sci. Technol.* 71(13), 1593-1599. DOI: 10.1016/j.compscitech.2011.07.003

Sokovnin, O. M., Zagoskina, N. V., and Zagoskin, S. N. (2015). "A study of the deep-bed filtration of a suspension of ash particles," *Theor. Found. Chem. Eng.* 49(5), 688-698. DOI: 10.1134/S0040579515040363

Svagan, A. J., Samir, M. A. S. A., and Berglund, L. A. (2008). "Biomimetic foams of high mechanical performance based on nanostructured cell walls reinforced by native cellulose nanofibrils," *Adv. Mater.* 20(7), 1263-1269. DOI: 10.1002/adma.200701215

Teagarden, D. L., and Baker, D. S. (2002). "Practical aspects of lyophilization using non-aqueous co-solvent systems," *Eur. J. Pharm. Sci.* 15(2), 115-133. DOI: 10.1016/S0928-0987(01)00221-4

Thiessen, R. J. (2006). "Filtration of respired gases: Theoretical aspects," *Respiratory Care Clinics of North America* 12(2), 183-201. DOI: 10.1016/j.rcc.2006.03.001

Vessot, S., and Andrieu, J. (2012). "A review on freeze drying of drugs with *tert*-butanol (TBA) + water systems: Characteristics, advantages, drawbacks," *Dry. Technol.* 30(4), 377-385. DOI: 10.1080/07373937.2011.628133

Wan, H., Wang, N., Yang, J., Si, Y., Chen, K., Ding, B., Sun, G., El-Newehy, M., Al-Deyab, S. S., and Yu, J. (2014). "Hierarchically structured polysulfone/titania fibrous membranes with enhanced air filtration performance," *J. Colloid Interf. Sci.* 417, 18-26. DOI: 10.1016/j.jcis.2013.11.009

Wang, J., Yuan, Y., Zhang, L., and Wang, R. (2009). "The influence of viscosity on stability of foamy oil in the process of heavy oil solution gas drive," *J. Petrol. Sci. Eng.* 66(1-2), 69-74. DOI: 10.1016/j.petrol.2009.01.007

Wang, T., Wang, N., Zhang, Y., Shen, W., Gao, X., and Li, T. (2010). "Solvent injection-lyophilization of tert-butyl alcohol/water cosolvent systems for the preparation of drug-loaded solid lipid nanoparticles," *Colloid. Surface. B* 79(1), 254-261. DOI: 10.1016/j.colsurfb.2010.04.005

Waschkies, T., Oberacker, R., and Hoffmann, M. J. (2011). "Investigation of structure formation during freeze-casting from very slow to very fast solidification velocities," *Acta Mater.* 59(13), 5135-5145. DOI: 10.1016/j.actamat.2011.04.046

Wittaya-Areekul, S., and Nail, S. L. (1998). "Freeze-drying of *tert*-butyl alcohol/water cosolvent systems: Effects of formulation and process variables on residual solvents," *J. Pharm. Sci.* 87(4), 491-495. DOI: 10.1021/js9702832

World Health Organization (2015). "Ambient (outdoor) air quality and health," (http://www.who.int/mediacentre/factsheets/fs313/en/), Accessed on 09.09.2016.

Wu, C.-F., Woodward, A., Li, Y.-R., Kan, H., Balasubramanian, R., Latif, M. T., Sahani, M., Cheng, T.-J., Chio, C.-P., Taneepanichskul, N., *et al*. (2017). "Regulation of fine particulate matter ($PM_{2.5}$) in the Pacific Rim: Perspectives from the APRU Global Health Program," *Air Qual. Atmos. Hlth.*, 1-11. DOI: 10.1007/s11869-017-0492-x

Yang, Y., Zhang, S., Zhao, X., Yu, J., and Ding, B. (2015). "Sandwich structured polyamide-6/polyacrylonitrile nanonets/bead-on-string composite membrane for effective air filtration," *Sep. Purif. Technol.* 152, 14-22. DOI: 10.1016/j.seppur.2015.08.005

Zamani, A., and Maini, B. (2009). "Flow of dispersed particles through porous media - Deep bed filtration," *J. Petrol. Sci. Eng.* 69(1-2), 71-88. DOI: 10.1016/j.petrol.2009.06.016

Zhao, F., Chu, H., Yu, Z., Jiang, S., Zhao, X., Zhou, X., and Zhang, Y. (2017). "The filtration and fouling performance of membranes with different pore sizes in algae harvesting," *Sci. Total Environ.* 587-588, 87-93. DOI: 10.1016/j.scitotenv.2017.02.035

Article submitted: April 22, 2018; Peer review completed: June 5, 2018; Revised version received: June 6, 2018; Accepted: June 7, 2018; Published: June 13, 2018.
DOI: 10.15376/biores.13.3.5894-5908